International Journal of Mass Spectrometry 279 (2009) 170–175

Contents lists available at ScienceDirect

International Journal of Mass Spectrometry

journal homepage: www.elsevier.com/locate/ijms

Short communication

Accurate characterization of carcinogenic DNA adducts using MALDI tandem time-of-flight mass spectrometry

Charles A. Barnes [1], Norman H.L. Chiu *

Department of Chemistry and Biochemistry, University of North Carolina at Greensboro, Greensboro, NC 27402, United States

ARTICLE INFO

Article history:
Received 21 July 2008
Received in revised form 7 October 2008
Accepted 10 October 2008
Available online 21 October 2008

Keywords:
DNA adducts
Collision-induced dissociation
MALDI
Tandem time-of-flight

ABSTRACT

Many chemical carcinogens and their *in vivo* activated metabolites react readily with genomic DNA, and form covalently bound carcinogen-DNA adducts. Clinically, carcinogen-DNA adducts have been linked to various cancer diseases. Among the current methods for DNA adduct analysis, mass spectroscopic method allows the direct measurement of unlabeled DNA adducts. The goal of this study is to explore the use of matrix-assisted laser desorption/ionization tandem time-of-flight mass spectrometry (MALDI-TOF/TOF MS) to determine the identity of carcinogen-DNA adducts. Two of the known carcinogenic DNA adducts, namely N-(2′-deoxyguanosin-8-yl)-2-amino-1-methyl-6-phenyl-imidazo [4,5-b] pyridine (dG-C8-PhIP) and N-(2′-deoxyguanosin-8yl)-4-aminobiphenyl (dG-C8-ABP), were selected as our models. In MALDI-TOF MS measurements, the small matrix ion and its cluster ions did not interfere with the measurements of both selected dG adducts. To achieve a higher accuracy for the characterization of selected dG adducts, 1 keV collision energy in MALDI-TOF/TOF MS/MS was used to measure the adducts. In comparison to other MS/MS techniques with lower collision energies, more extensive precursor ion dissociations were observed. The detection of the corresponding fragment ions allowed the identities of guanine, PhIP or ABP, and the position of adduction to be confirmed. Some of the fragment ions of dG-C8-PhIP have not been reported by other MS/MS techniques.

1. Introduction

Despite the continuous efforts in cancer research, cancer still remains as a major health problem worldwide today. In the US, cancer is the second leading cause of death. Chemicals that can potentially lead to the development of cancer diseases are classified as carcinogens. Some carcinogens and their *in vivo* activated metabolites have shown to be reactive with deoxyribonucleic acid (DNA), and form covalently bound carcinogen-DNA adducts. Many carcinogen-DNA adducts have been used as toxicogenomics biomarkers to monitor the exposure of individuals to specific carcinogens in our diets or living environment [1–3]. Clinically, different carcinogen-DNA adducts have been linked to cancer diseases. Among the carcinogen-DNA adducts that have been isolated and characterized from *in vitro* and *in vivo* studies, N-(2′-deoxyguanosin-8-yl)-2-amino-1-methyl-6-phenyl-imidazo [4,5-b] pyridine (dG-C8-PhIP) and N-(2′-deoxyguanosin-8yl)-4-aminobiphenyl (dG-C8-ABP) represent the most abundant and potent adducts in the categories of heterocyclic aromatic amines and aromatic amines DNA adducts, respectively [4–6]. Both adducts have been associated with more than one type of cancer diseases [6–8]. 2-Amino-6-phenyl-1-methylimidzao [4,5-b] pyridine (PhIP) is found in tobacco smoke. PhIP can also be generated from cooking meats. Following the intake of PhIP, the compound is activated by P450 enzymes, and reacts with DNA and other biomolecules. In the case of DNA, the activated PhIP reacts predominantly with 2′-deoxyguanosine (dG) and forms dG-PhIP adduct. Most, but not all, of the DNA adducts in the genome are normally removed by the DNA repair mechanisms. Any unrepaired DNA adducts can potentially lead to genetic mutation when the genome is replicated. Hence, the accuracy on monitoring DNA adduction is crucial to a variety of clinical and non-clinical studies. For 4-aminobiphenyl (ABP), the chemical has been found in tobacco smoke, hair dyes, and so on [9]. The *in vivo* activation and adduction of ABP are very similar to the chemistry of PhIP.

Among the current methods for measuring carcinogen-DNA adducts, the most common approach begins with the reduction of the genome to its monomeric units, i.e., deoxyribonucleosides (dN). Specific digestion of a genome can be achieved by using the enzy-

* Corresponding author at: Department of Chemistry and Biochemistry, University of North Carolina at Greensboro, 410 Sullivan Science Building, 301 McIver Street, Greensboro, NC 27412, United States. Tel.: +1 336 334 3126.
E-mail address: nhchiu@uncg.edu (N.H.L. Chiu).
[1] Current address : Department of Chemistry, Iowa State University, Ames, IA 50011, United States.

1387-3806/$ – see front matter © 2008 Elsevier B.V. All rights reserved.
doi:10.1016/j.ijms.2008.10.006

matic activity of nucleases, e.g., DNase I, whose activities are not usually affected by the presence of carcinogen-DNA adducts [10]. The ratio of unmodified dN to DNA adducts in the human genome is estimated to be as high as 10^9 [11]. For this reason, after digesting the genome, the removal of unmodified dN would greatly facilitate the specific detection of DNA adducts. The separation of digested deoxyribonucleoside mixture is often achieved by using either liquid chromatography or capillary electrophoresis. To monitor the continuous flow of eluent from a separation column, electrospray ionization (ESI) mass spectrometers that are equipped with a transmission mass analyzer, e.g., triple quadrupole and ion trap, have been commonly used to detect DNA adducts [11,12]. With the recent success on both off-line and on-line coupling of liquid chromatography techniques to matrix-assisted laser desorption/ionization mass spectrometry (MALDI MS), the use of MALDI MS has become a viable approach for DNA adduct analysis [13–15]. In general, as little as a few nanoliter of sample is required for MALDI MS measurements [16–18]. The sampling rate of MALDI samples has recently been improved to meet the demands in high throughput analysis [19]. In this report, the use of MALDI tandem time-of-flight MS to accurately determine the identity of carcinogenic DNA adducts is explored. To demonstrate the feasibility of using MALDI-TOF/TOF MS, two different categories of DNA adducts, namely dG-C8-PhIP and dG-C8-ABP adducts, were used as the models in this study.

2. Experimental

2.1. Materials

N-(2′-deoxyguanosin-8-yl)-2-amino-1-methyl-6-phenylimidazo [4,5-b] pyridine and N-(2′-deoxyguanosin-8yl)-4-aminobiphenyl were obtained from Toronto Research Chemicals Inc. (Toronto, Canada). 2′-deoxyguanosine monohydrate (dG_{OH}) 99%, 3-hydroxypicolinic acid (3-HPA) MALDI matrix was purchased from Sigma–Aldrich (St. Louis, MO). Anhydrous N,N-dimethylformamide (DMF) 99.8% was purchased from Acros Organics (Geel, Belgium). 2′,4′,6′-trihydroxyacetophenone monohydrate (THAP) MALDI matrix, and ammonium citrate dibasic ≥99.0% was purchased from Fluka (Buchs, Switzerland). Acetonitrile HPLC grade, and methanol HPLC grade were obtained from Fisher Scientific (Pittsburgh, PA). Non-sterile 0.22 μm low protein binding Durapore (PVDF) syringe driven membrane filter units (25 mm) were purchased from Millipore Corp. (Bedford, MA).

2.2. MALDI matrix solution and sample preparation method

The 3-HPA matrix solution was prepared by dissolving 35.0 mg of 3-HPA and 8.80 mg of ammonium citrate dibasic in 1.0 mL of 10% acetonitrile. The THAP matrix solution was prepared by dissolving 10.0 mg of THAP and 9.80 mg of ammonium citrate dibasic in 1.0 mL of 50% acetonitrile. After vortexing the matrix solutions for 1–2 min, any undissolved particles were removed by filtering the matrix solutions with 0.22 μm membrane filter. The matrix solutions were stored at −20°C.

All DNA samples were dissolved in DMF, and were freshly diluted in DMF. The MALDI samples were prepared by the thin-layer method. After cleaning the stainless steel MALDI sample plate with deionized water and methanol, 0.3 μL of a matrix solution was spotted on the MALDI sample plate. The matrix was allowed to air dry. 0.3 μL of 1 mM DNA sample was then spotted over the dried matrix, and the mixture was allowed to air dry.

2.3. MALDI-TOF MS measurements

A MALDI-TOF/TOF instrument (4700 Proteomics Analyzer, Applied Biosystems, Framingham, MA) was used for all MS and MS/MS measurements. Each sample was measured by using the linear low mass positive mode in the 4000 Series Explorer Version 3.0 software. The Nd:YAG laser (200 Hz) was set at 4000 a.u. (maximum setting = 7900 a.u.). The focus mass was the mass of an expected molecular ion from each sample. Molecular ions were extracted from the ion source after 400 ns delay with the low mass gate being turned off. The accelerating voltage was +20.0 kV and grid voltage was +18.8 kV. The instrument was equipped with a 200 Hz digitizer. The sampling bin size was 0.5 ns with an input bandwidth of 500 MHz, and a vertical full scale of 500 mV. The linear detector voltage was +2.0 kV. The pressure inside the entire instrument was maintained at the level of 10^{-8} Torr. Each spectrum was automatically acquired by accumulating the results of 3000 shots (50 shots per sub-spectrum) with random edge-biased positioning of each laser shot. By using the Data Explorer Version 4.6 software, resulting mass spectrum was internally calibrated with the peak of $[3\text{-HPA} + H]^+$ ion (140.0 Da), except the spectrum obtained from 3-HPA alone. For post-source decay (PSD) measurements, the same parameter settings as the MS/MS measurements described below were used, except the pressure inside the collision cell was maintained at 10^{-8} Torr.

2.4. MALDI-TOF/TOF MS/MS measurements

Each sample was measured by using the MS–MS 1 kV positive mode in the 4000 Series Explorer Version 3.0 software. Higher laser intensity at 6000 a.u. was used. The precursor mass was the molecular mass of selected DNA adducts, and the mass window was −1.00 Da and +5.00 Da of precursor mass. Molecular ions were extracted from the ion source after 460 ns delay. The suppressor for metastable ion was turned off. The accelerating voltage at the ion source was at +8.0 kV, and grid voltage at +6.85 kV. The collision cell was at +7.0 kV. Fragment ions were extracted from the collision cell after 27.3 ms delay. The accelerating voltage from the collision cell was at +15.0 kV. The sampling bin size was 0.5 ns with an input bandwidth of 500 MHz, and a vertical full scale of 200 mV. The reflector detector voltage was +2.1 kV. The pressure inside the collision cell was adjusted with atmospheric gas to the level of 10^{-6} Torr before the measurements were carried out. Each spectrum was automatically acquired by accumulating the results of 5000 shots (125 shots per sub-spectrum) with random edge-biased positioning of each laser shot. By using the Data Explorer Version 4.6 software, resulting mass spectrum was internally calibrated with the most abundant isotopic peaks of precursor ion and a known fragment ion. ChemSketch version 8.17 software was used for drawing the molecular structures, and Mass Spec Calculator Professional demo version 4.09 software was used to assist the identification of the fragment ions.

3. Results and discussion

For MALDI mass spectrometry of DNA, 3-HPA is one of the most commonly used MALDI matrices. In an initial experiment, 3-HPA matrix was measured by using the linear positive mode in MALDI-TOF MS. The peak corresponded to $[3\text{-HPA} + H]^+$ ($140.0\ m/z$) was detected as shown in Fig. 1(a). Many MALDI matrices, including 3-HPA, are known to form multiple matrix cluster ions during the MALDI process. In Fig. 1(a), some of the positively charged 3-HPA matrix cluster ions were detected. Normally, the matrix ion together with its cluster ions is removed by using a low mass ion

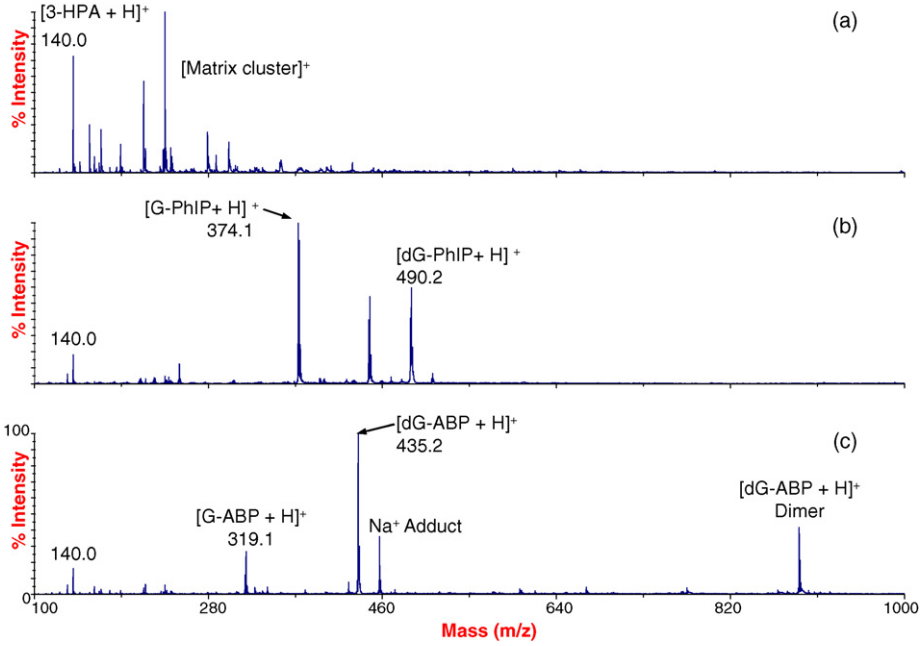

Fig. 1. MALDI-TOF MS spectra of (a) 3-HPA alone, (b) dG-C8-PhIP with 3-HPA matrix, and (c) dG-C8-ABP with 3-HPA matrix. G-PhIP and G-ABP correspond to fragment ions without the 2′-deoxyribose in dG-C8-PhIP and dG-C8-ABP, respectively. All measurements were carried out in the linear positive ion mode.

gate in the MALDI-TOF instrument. As shown in Fig. 1(a), most of the 3-HPA matrix cluster ions were less than 300 *m*/*z*. For this reason, both 3-HPA matrix ion and its cluster ions did not interfere with the MALDI-TOF MS measurements of both selected 2′-deoxyguanosine adducts as demonstrated in Fig. 1, thus allowing the correct selection of dG adduct precursor ions for MS/MS measurements. In both Fig. 1(b) and (c), a less intense peak next to the dG adduct ion peak with a mass difference of 1 Da is identified as the loss of a hydrogen radical from the dG adduct ion. The loss of hydrogen radical could be the result of using relatively high concentration (1 mM) of dG adducts, and/or laser-induced fragmentation of dG adducts during the MALDI process. An alternative MALDI matrix for DNA measurements, namely THAP, was used separately to prepare both dG adduct samples. Despite less THAP matrix cluster ions were observed, more aglycon ions were produced (data not shown). To facilitate the subsequent MS/MS measurements of dG adducts, the in-source fragmentation of dG adduct ions ought to be minimized. Hence, 3-HPA matrix was chosen for the rest of this study. In Fig. 1(b) and (c), the peak that corresponds to the aglycon ion of each dG adduct is detected. The same aglycon ions have been reported when electrospray ionization MS was used to measure dG adducts [20,21]. In the case of MALDI-TOF MS, the N-glycosidic bond between guanine and 2′-deoxyribose was broken by an excessive transfer of laser energy to dG adduct during the MALDI process [22]. Also, the preparation of MALDI samples required mixing each adduct with acidic 3-HPA matrix (pH 3), which could hydrolyze some of the dG adducts [23]. Despite the mass accuracy that can be achieved by MALDI-TOF MS, the identities of guanine, and PhIP or ABP in the dG adducts remain uncertain. Furthermore, it is important to ensure the selected carcinogens have specifically reacted with guanine at the C8 position. This is because different dG adduct isomers have been identified, and shown to have different effects on the mechanisms of DNA repair and/or transcription.

Recently, Debrauwer and co-workers have reported the sequential MS^3 measurement of dG-C8-PhIP by using the latest collision-induced dissociation (CID) technology of an ion trap [24]. With sub-ppm mass accuracy, all the fragment ions from the MS^3 spectrum of dG-C8-PhIP were identified. Multiple fragment ions were originated from the guanine moiety of dG-C8-PhIP, thus confirming the identity of the nucleobase. The identity of the dG adduct C8 isomer was also confirmed by other fragment ions. None of the fragment ions, however, corresponded to the dissociation of the PhIP moiety. For the purpose of distinguishing dG-C8-PhIP adduct from other possible dG adducts, it is important to obtain MS/MS data from the dissociation of the PhIP moiety. Independently, by using the same MS/MS technique, Turesky and co-workers have also reported the sequential MS^3 measurement of dG-C8-PhIP [25]. The results have shown an identical pattern of fragment ions in the MS^3 spectrum of dG-C8-PhIP as reported by Debrauwer and co-workers. Turesky's report has also included a MS^4 spectrum of the most abundant fragment ion (357 *m*/*z*) obtained from the MS^3 measurement, which was identified as G-PhIP ion without the primary amine group at the C2 position of guanine. No fragment ion corresponded to the dissociation of the PhIP moiety was identified in the MS^4 spectrum of dG-C8-PhIP. Shields and co-workers have analyzed dG-C8-PhIP 5′-monophosphate that has been enzymatically released from a modified oligodeoxynucleotide by using the post-source decay in MALDI-TOF MS [26]. A unique fragment ion (167 *m*/*z*) that corresponded to PhIP ion without the primary amine group at the C2 position of PhIP was identified in their PSD spectrum. In comparison to the CID experiments described above, the metastable ion of dG-C8-PhIP 5′-monophosphate generated by the MALDI ion source did not yield sufficient fragmentation, thus limited the accuracy on identifying the dG adduct.

In comparison to the conventional MALDI-TOF instruments that are equipped with reflectron for performing PSD measurements, the instrumental design in a MALDI-TOF/TOF instrument allows PSD measurements to be carried out in a slightly different approach. In brief, metastable ions from the MALDI ion source are channeled through the first time-of-flight (TOF) analyzer and entered a virtually empty collision cell at 10^{-8} Torr, which is co-axially located in between the first and second TOF analyzer. After allowing the ions to undergo fragmentation within the collision cell, the fragment ions are extracted into the second TOF analyzer where the

ions are separated. As part of a preliminary study in this report, the selected dG adducts were characterized separately by using PSD in the MALDI-TOF/TOF instrument. With higher laser intensity than the threshold value for MALDI-TOF MS measurements, no fragment ions were observed from the PSD measurements, except the corresponding aglycon ion from each dG adduct (data not shown).

To achieve a higher accuracy, the rest of this study focuses on using the high energy CID in MALDI-TOF/TOF to characterize the selected DNA adducts. Similar to the PSD measurements, the MS/MS measurements in MALDI-TOF/TOF required the use of optimal DNA adduct concentration in the sample and laser intensity to generate sufficient precursor ions. The key, however, was the air pressure within the collision cell. When the CID pressure was increased to 10^{-6} Torr, extensive and reproducible fragmentation of dG-C8-PhIP precursor ion was observed (Fig. 2). To ensure adequate mass accuracy was attained, the dG-C8-PhIP precursor ion (490.2 m/z) and a known fragment ion (250.1 m/z) of dG-C8-PhIP were chosen as internal calibrants. For both internal calibrants, the highest isotopic peak was selected as the most abundant carbon-12 isotope. In the case of the internal calibrant at 250.1 m/z, the identities of the peaks that correspond to various isotopes of fragment ion, *D*, are confirmed by their expected signal intensities as shown in Fig. 2. For identifying the precursor ion peak at 490.2 m/z, the unlabeled peaks on the left hand side immediately next to the highest isotopic peak all have a mass difference of −1 Da. These smaller unlabeled peaks could correspond to the loss of one and more than one hydrogen radicals from the precursor ion as a result of using high energy (1 keV) collision-induced dissociation to fragment the precursor ion [27]. The hypothesis on the loss of hydrogen radicals from the dG-C8-PhIP precursor ion is supported by the results of measuring 2′-deoxyguanosine monohydrate (dG_{OH}) under the same conditions of high energy collision-induced dissociation. Comparatively, the fragmentation pattern of dG_{OH} ion in Fig. 3 is similar to the one obtained from dG-C8-PhIP. Next to the dG_{OH} precursor peak in Fig. 3, there are also multiple less intense peaks with mass differences of −1 Da that correspond to the loss of hydrogen radicals. In Fig. 2, by using the two-point internal calibration and identify the labeled fragment ions (A–F) with the highest isotopic peaks as their corresponding carbon-12 isotopes, <24 ppm average mass accuracy was achieved. The mass accuracy of each fragment ion was determined by comparing the measured molecular mass to its theoretical molecular mass. The identities for some of the fragment ions (A, B, and D) and their relative abundance in Fig. 2 comply with the results of earlier reports, in which different tandem MS techniques were used to fragment the same dG-C8-PhIP ion [24,25]. To the best of our knowledge, the fragment ions (C, E, and F) of dG-C8-PhIP in Fig. 2 were never observed by using other tandem MS techniques. Based on the results in Fig. 2, it indicates both guanine and PhIP moieties of dG-C8-PhIP are dissociated at multiple positions. Thus, the detection of the fragment ions (A–F) allows us to confirm the identities of guanine and PhIP and, the position of PhIP adduction at the C8 position of guanine. Together with the results from the MS measurement shown in Fig. 1(b), the accuracy on identifying the dG-C8-PhIP is improved by using the MALDI-TOF/TOF tandem MS technique.

To demonstrate the applicability of MALDI-TOF/TOF tandem MS technique for DNA adduct analysis, the same method was used to characterize dG-C8-ABP adduct. The results showed the same level of accuracy could be achieved (Fig. 4). Both guanine and ABP moieties were dissociated at multiple positions, thus allowing the identification of guanine, ABP, and the position of ABP adduction to be accomplished. Similarly, a two-point mass calibration was preformed with the data obtained from the MS/MS measurement of dG-C8-ABP. The average mass accuracy of the identified fragment ions in Fig. 4 was also below 24 ppm.

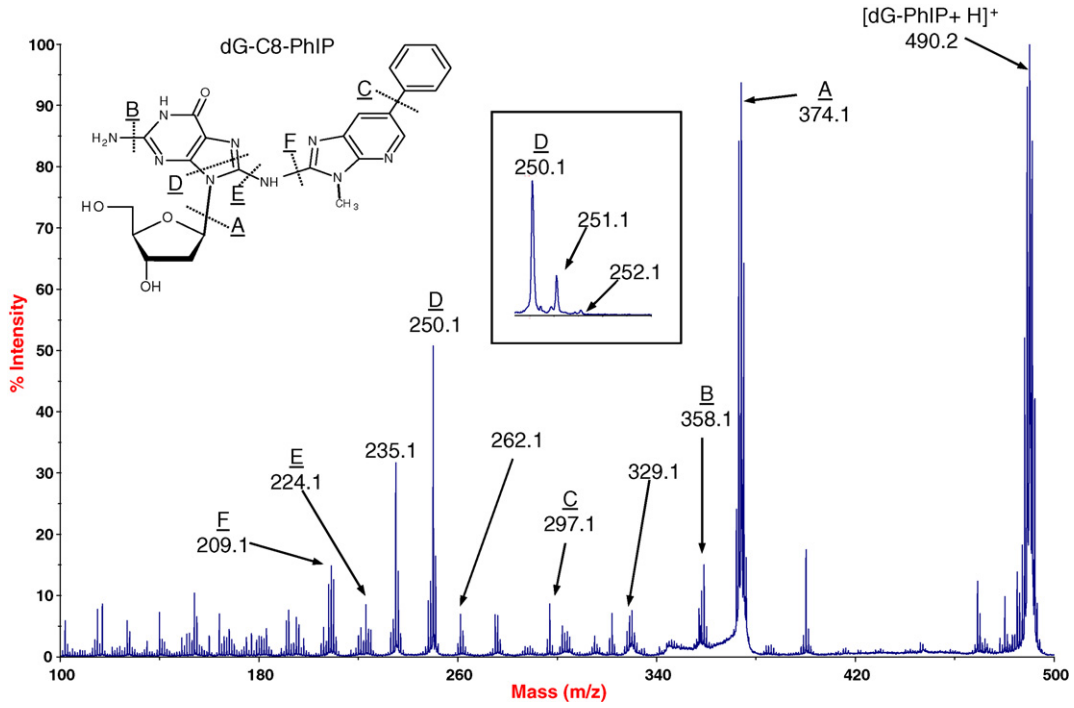

Fig. 2. MS/MS spectrum of dG-C8-PhIP in the positive ion mode. The precursor ion of 490.2 m/z was selected for the MS/MS measurement. A two-point internal mass calibration was performed by using the highest isotopic peak of the precursor ion (490.2 m/z) and a known dG-C8-PhIP fragment ion (250.1 m/z) as shown in the inserted spectrum. Peaks A–F correspond to fragment ions of dG-C8-PhIP, whose identities are shown in the inserted molecular structure of dG-C8-PhIP. The dotted lines in the molecular structure of dG-C8-PhIP represent the positions of dissociation that would produce the corresponding fragment ions. All the other labeled peaks correspond to fragment ions that were previously reported in Refs. [24,25]. All the measured molecular masses were determined with their highest isotopic peaks.

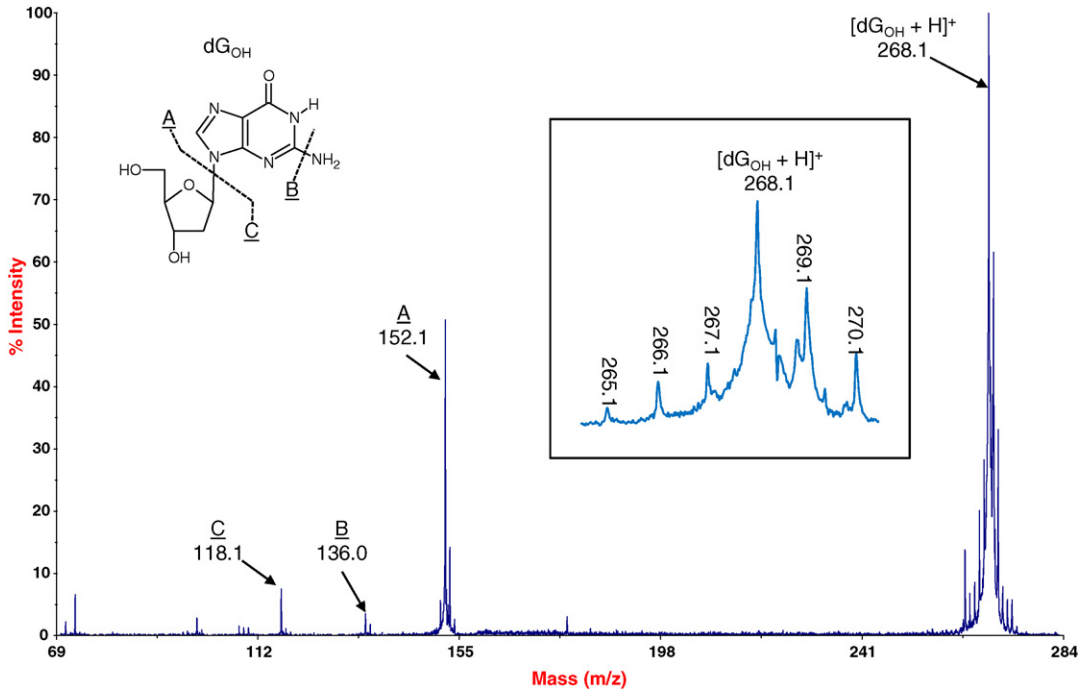

Fig. 3. MS/MS spectrum of 2′-deoxyguanosine monohydrate (dG$_{OH}$) in the positive ion mode. The precursor ion of 268.1 m/z was selected for the MS/MS measurement. An internal mass calibration was performed by using the highest isotopic peak of the precursor ion. Peaks A–C correspond to fragment ions of dG$_{OH}$, whose identities are shown in the inserted molecular structure of dG$_{OH}$. The dotted lines in the molecular structure of dG$_{OH}$ represent the positions of dissociation that would produce the corresponding fragment ions. All the measured molecular masses were determined with their highest isotopic peaks.

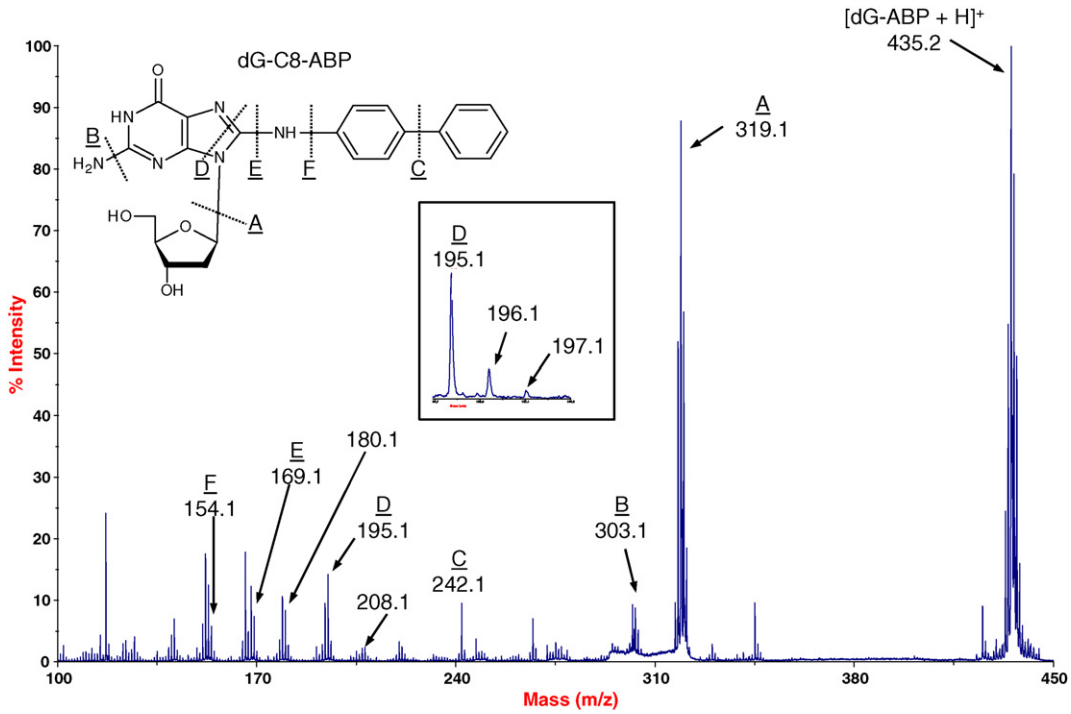

Fig. 4. MS/MS spectrum of dG-C8-ABP in the positive ion mode. The precursor ion of 435.2 m/z was selected for the MS/MS measurement. A two-point internal mass calibration was performed by using the highest isotopic peak of the precursor ion (435.2 m/z) and a known dG-C8-ABP fragment ion (195.1 m/z) as shown in the inserted spectrum. Peaks A–F correspond to fragment ions of dG-C8-ABP, whose identities are shown in the inserted molecular structure of dG-C8-ABP. The dotted lines in the molecular structure of dG-C8-ABP represent the positions of dissociation that would produce the corresponding fragment ions. All the other labeled peaks correspond to fragment ions that were previously reported in Refs. [21,28]. All the measured molecular masses were determined with their highest isotopic peaks.

4. Conclusions

As far as we are concerned, this report is the first attempt on using MALDI-TOF/TOF MS/MS to perform the qualitative analysis of carcinogenic DNA adducts. In both cases of dG-C8-PhIP and dG-C8-ABP adduct, the use of higher collision energy has led to more extensive precursor ion dissociations. Three of the fragment ions obtained from dG-C8-PhIP have not been reported by other MS/MS techniques. The results have accurately confirmed the identities of guanine, PhIP or ABP moiety, and the position of adduction by more than one of their corresponding fragment ions. Together with the signals that corresponded to the molecular dG adduct ions, the accuracy on using MALDI tandem time-of-flight mass spectrometry to characterize the selected carcinogenic DNA adducts should meet the highest analytical standard for both clinical and non-clinical studies on DNA adduction. Equally important, with the high repetitive UV laser ($\geq$200 Hz), the rate of sample throughput of MALDI-TOF/TOF is expected to meet the requirements of large-scale studies in the future.

Acknowledgements

The authors wish to thank Nadja Cech and Liam Duffy for helpful discussion. CAB wishes to acknowledge the Undergraduate Research Assistantship received from the Office of Undergraduate Research at UNCG. All other financial supports were received from Department of Chemistry and Biochemistry and College of Arts and Science at UNCG. The MALDI-TOF/TOF instrument was purchased with a NSF Major Research Instrumentation Grant (Award #0420292).

References

[1] D.H. Phillips, Mutat. Res. 577 (2005) 284.
[2] A. Rundle, Mutat. Res. 600 (2006) 23.
[3] H. Frandsen, S. Grivas, R. Anderson, L. Dragsted, J.C. Larsen, Carcinogenesis 13 (1992) 629.
[4] D. Lin, K.R. Kaderlik, R.J. Turesky, D.W. Miller, J.O. Lay, F.F. Kadlubar, Chem. Res. Toxicol. 5 (1993) 691.
[5] F.A. Beland, D.R. Doerge, M.I. Churchwell, M.C. Poirier, B. Schoket, M.M. Marques, Chem. Res. Toxicol. 12 (1999) 68.
[6] J. Zhu, P. Chang, M.L. Bondy, A.A. Sahin, S.E. Singletary, S. Takahashi, T. Shirai, D. Li, Cancer Epidemiol. Biomarkers Prev. 12 (2003) 830.
[7] D. Tang, J.J. Liu, A. Rundle, C. Neslund-Dudas, A.T. Savera, C.H. Bock, N.L. Nock, J.J. Yang, B.A. Rybicki, Cancer Epidemiol. Biomarkers Prev. 16 (2007) 803.
[8] B. Zayas, S.W. Stillwell, J.S. Wishnok, L.J. Trudel, P. Skipper, M.C. Yu, S.R. Tannenbaum, G.N. Wogan, Carcinogenesis 28 (2007) 342.
[9] R.J. Turesky, J.P. Freeman, R.D. Holland, D.M. Nestorick, D.W. Miller, D.L. Ratnasinghe, F.F. Kadlubar, Chem. Res. Toxicol. 16 (2003) 1162.
[10] L. Qing, N.H.L. Chiu, P. Vouros, Anal. Chem. 79 (2007) 1907.
[11] R. Singh, P.B. Farmer, Carcinogenesis 27 (2006) 178.
[12] E.M. Ricicki, C.L. Andrews, S. Schiavo, P. Vouros, Analysis of DNA Adducts: The Encyclopedia of Mass Spectrometry, vol. 3, Elsevier, Oxford, 2006.
[13] J. Preisler, F. Foret, B.L. Karger, Anal. Chem. 70 (1998) 5278.
[14] V.C. Chen, K. Cheng, W. Ens, K.G. Standing, J.I. Nagy, H. Perreault, Anal. Chem. 76 (2004) 1189.
[15] K.S. Marcus, H. Schaefer, S. Klaus, C. Bunse, R. Swart, H.E. Meyer, J. Proteome Res. 6 (2007) 636.
[16] D.P. Little, T.J. Cornish, M.L. O'Donnell, A. Braun, R.J. Cotter, H. Koester, Anal. Chem. 69 (1997) 4540.
[17] G. Allmaier, Rapid Commun. Mass Spectrom. 11 (1997) 1567.
[18] H. Zhang, K.K.C. Yeung, Anal. Chem. 76 (2004) 6814.
[19] E. Moskovets, J. Preisler, H.S. Chen, T. Rejtar, V. Andreev, B.L. Karger, Anal. Chem. 78 (2006) 912.
[20] D. Rindgen, R.J. Turesky, P. Vouros, Chem. Res. Toxicol. 8 (1995) 1005.
[21] E.M. Ricicki, J.R. Soglia, C. Teitel, R. Kane, F. Kadlubar, P. Vouros, Chem. Res. Toxicol. 18 (2005) 692.
[22] V. Gabelica, E. Schulz, M. Karas, J. Mass Spectrom. 39 (2004) 579.
[23] J.A. Zoltewicz, D.F. Clark, T.W. Sharpless, G. Grahe, J. Am. Chem. Soc. 92 (1970) 1741.
[24] E.L. Jamin, D. Arquier, C. Canlet, E. Rathahao, J. Tulliez, L. Debrauwer, J. Am. Soc. Mass Spectrom. 18 (2007) 2107.
[25] A.K. Goodenough, H.A. Schut, R.J. Turesky, Chem. Res. Toxicol. 20 (2007) 263.
[26] K. Brown, C.A. Harvey, K.W. Turteltaub, S.J. Shields, J. Mass Spectrom. 38 (2003) 68.
[27] L. Nizigiyimana, P.K. Rajan, A. Haemers, M. Claeys, P.J. Derrick, Rapid Commun. Mass Spectrom. 11 (1997) 1808.
[28] D.R. Doerge, M.I. Churchwell, M.M. Marques, F.A. Beland, Carcinogenesis 20 (1999) 1055.